Front. Mater. Sci. 2013, 7(2): 196–201
DOI 10.1007/s11706-013-0198-4

COMMUNICATION

Structural, optical and electron paramagnetic resonance studies on Cu-doped ZnO nanoparticles synthesized using a novel auto-combustion method

R. ELILARASSI (✉) and G. CHANDRASEKARAN

Magnetism and Nanomagnetic Materials Lab, Department of Physics, School of Physical, Chemical and Applied Sciences, Pondicherry University, Puducherry 605014, India

ABSTRACT: Nanocrystalline $Zn_{1-x}Cu_xO$ (x = 0, 0.02, 0.04, 0.06, 0.08) samples were synthesized by a novel auto-combustion method using glycine as the fuel material. The structural, optical and magnetic properties of the samples were characterized using XRD, SEM, photoluminescence (PL) and electron paramagnetic resonance (EPR) spectroscopies. The XRD spectra of samples reveal the hexagonal wurtzite structures of ZnO. As the copper content increases, a diffraction peak at 2θ = 39° corresponding to secondary phase of CuO ([111] crystalline face) appears when $x \leqslant 6$ mol.%. PL spectra of the samples show a strong ultraviolet (UV) emission and defect related visible emissions. Cu-doping in ZnO can effectively adjust the energy level in ZnO, which leads to red shift in the emission peak position in UV region. The EPR spectra of Cu-doped ZnO nanoparticles show a distinct and broad signal at room temperature, suggesting that it may be attributed to the exchange interactions within Cu^{2+} ions.

KEYWORDS: Cu-doped ZnO; auto-combustion; luminescence; electron paramagnetic resonance (EPR)

Transition metal-doped semiconductor nanoparticles have been investigated extensively due to their excellent fluorescence properties for technological applications [1]. ZnO is an II–VI semiconductor with wide band gap (3.37 eV) and large exciton binding energy (60 meV) that has received a great deal of attention due to its potential applications in photonics and optoelectronic devices [2–5]. Transition metal doping in ZnO is an efficient method to tune the energy levels and surface states, which results in the interesting properties of nanostructured ZnO [6–7]. ZnO doped with transition metal is a room-temperature diluted magnetic semiconductor (DMS) exhibiting attractive magnetic, optical and electronic properties into a single substance [8–10]. Copper-doped zinc oxides exhibit ferromagnetic behavior and copper acts as a luminescence activator and compensator for an n-type material [11–12].

Though, several preparation methods namely the noble methods have been used to synthesize the nanostructured ZnO material that requires complex equipment and complicated operation, still it is a great challenge to synthesize metal oxide nanoparticles with high yield through a simple route. Herein, we report a simple novel auto-combustion method to prepare Cu-doped ZnO nanoparticles. The present method has several advantages, such as cost effective, easy to prepare metal oxide nanoparticles, high yield of the product, requiring low

Received November 27, 2012; accepted February 21, 2013

E-mail: ezhil1984_r@yahoo.co.uk

temperature, and the reaction is safe and quick [13]. In this study, we have prepared the various concentrations of Cu-doped ZnO nanoparticles by a simple and novel auto-combustion method. The structural, optical emission and electron paramagnetic resonance (EPR) properties of the Cu-doped ZnO nanoparticles annealed at 500°C were investigated in detail.

Nanocrystalline $Zn_{1-x}Cu_xO$ (x = 0, 0.02, 0.04, 0.06, 0.08) powder samples were synthesized by a simple and novel auto-combustion method using glycine as the combustion agent. Figure 1 shows the schematic diagram of the auto-combustion method. In the present synthesis of $Zn_{1-x}Cu_xO$ (x = 0, 0.02, 0.04, 0.06, 0.08), appropriate proportions of metal nitrates of $Zn(NO_3)_2 \cdot 6H_2O$, $Cu(NO_3)_2 \cdot 6H_2O$ and glycine ($C_2H_5NO_2$) were mixed without the addition of water. In the above mixture, a molar ratio of metal ion/glycine (1:1) was used. The aqueous solution was then stirred for about half an hour in order to mix the solution uniformly. The subsequent stage of heating of precursor resulted in repeated cycles of swelling and foaming accompanied with a strong self-propagating combustion reaction. Finally, a reticular substance obtained was ground well in an agate mortar for 1 h to get the powder of our interest. Then the resultant powder was annealed at 500°C and was used for further characterization studies.

The structure and phase purity of the powder samples were examined on an X-ray power diffractmeter (PAnalytical Model: X′Pert PRO). Scanning electron microscopy (SEM; HITACHI Model: S-3400N) was used to observe the microstructure of the resulting powders. Room-temperature photoluminescence (PL) studies were carried out using a spectrofluorimeter (Fluorolog-3). EPR measurements were carried out using EPR spectrograph (Jeol-100, X-Band).

The crystal structure of Cu-doped ZnO nanoparticles was investigated using X-ray diffraction (XRD) technique. Figure 2 shows the XRD patterns of $Zn_{1-x}Cu_xO$ (x = 0, 0.02, 0.04, 0.06, 0.08) nanoparticles annealed at 500°C. All the samples show the diffraction peaks corresponding to the hexagonal wurtzite structure of ZnO (JCPDS card No. 36-1451). Within the sensitivity of XRD instrument, no trace of copper metals, oxides, or any binary zinc copper phases is detected when the copper concentration is $\leqslant$4 mol.%. A diffraction peak at $2\theta = 39°$ corresponding to the secondary phase of CuO ([111] crystalline face) appears as

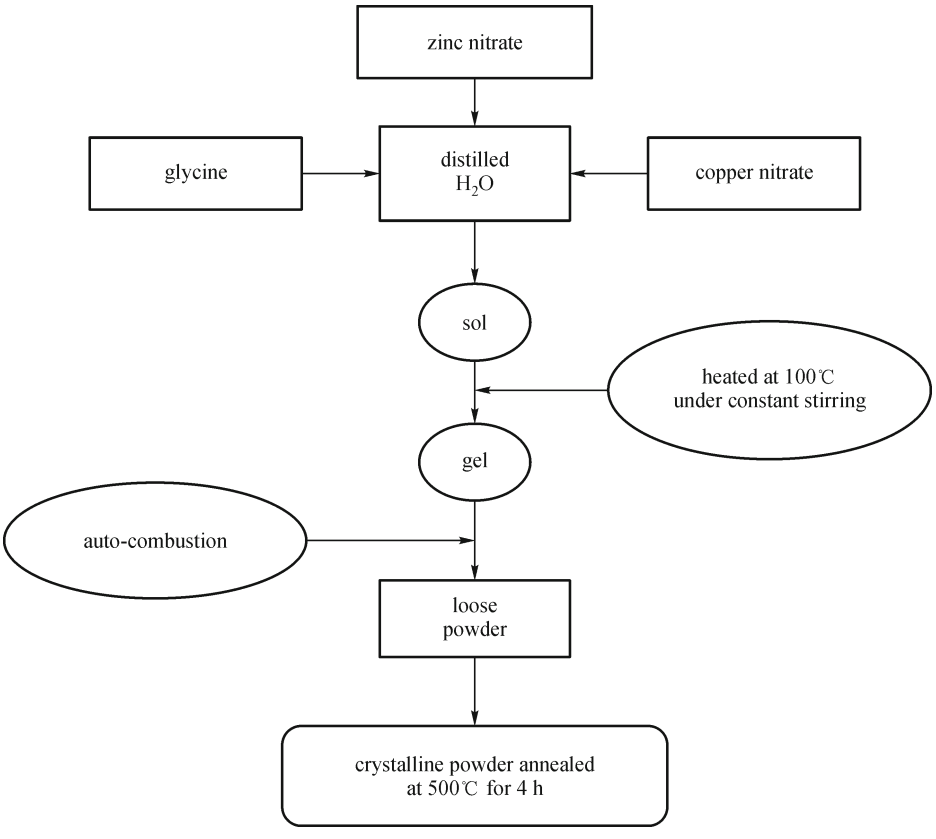

Fig. 1 A schematic diagram of the auto-combustion method.

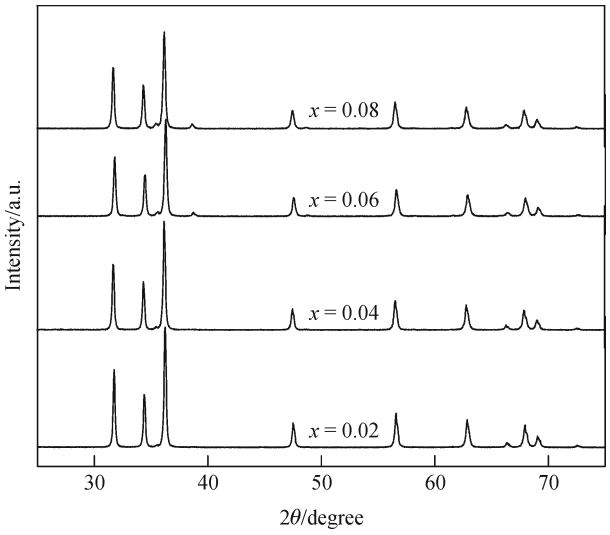

Fig. 2 XRD patterns of Cu-doped ZnO nanoparticles annealed at 500°C.

the copper content in ZnO is ⩾ 6 mol.%. In general, the incorporation of 3d-transition-metal ions deteriorates the crystallinity of ZnO due to their low solubility and various valence states [14]. Lee et al. reported that the thermal solubility limit of Cu in ZnO is below 5 mol.% [15]. The appearance of the CuO phase in samples ($x \geqslant 0.06$) means that the copper oxide was produced due to the limited solid solubility of Cu in the ZnO solvent. Hence, it is well understood from the segregation of a secondary phase that the thermal solubility limit of Cu in ZnO seems to be below 6 mol.% in our experiment settings.

The average particle size of Cu-doped ZnO powders is estimated from X-ray line broadening using the Debye–Scherrer equation:

$$D_{h,k,l} = \frac{0.9\lambda}{\Delta\theta\cos\theta} \tag{1}$$

where, D is the average crystallite diameter, λ is the wavelength of X-ray radiation, $\Delta\theta$ is the full width at half maximum (FWHM), and θ is the Bragg angle. Table 1 reveals that the average particle size decreases with increasing the copper content in ZnO. The lattice parameters a and c of the samples can be calculated using the formula as follows:

$$\sin^2\theta = \frac{\lambda^2}{4}\left[\frac{4}{3}\left(\frac{h^2+hk+k^2}{a^2}\right)+\frac{l^2}{c^2}\right] \tag{2}$$

where, θ is the diffraction angle, λ is incident wavelength (λ = 0.15406 nm), and h, k and l are all Miller's indices. The lattice parameters of the Cu-doped ZnO nanoparticles give values which show larger values from that pure a = 3.249 Å and c = 5.205 Å (JCPDS card No. 36-1451). Table 1 apparently results from the substitution of copper ions with a larger ionic radius of 0.96 Å compared with 0.74 Å of zinc ions [16]. The sample was characterized using SEM to investigate the morphology. Figure 3 shows the SEM image of the $Zn_{0.92}Cu_{0.08}O$ sample annealed at 500°C. The SEM image clearly reveals the presence of randomly distributed spherical shaped nanoparticles.

Table 1 Particle size and lattice parameters of Cu-doped ZnO samples annealed at 500°C

Copper concentration, x	Particle size /nm	Lattice parameters	
		a/Å	c/Å
0.02	46.97	3.2527±0.0017	5.2096±0.0005
0.04	43.14	3.2545±0.0035	5.2128±0.0008
0.06	39.05	3.2509±0.0020	5.2087±0.0006
0.08	22.21	3.2531±0.0032	5.2136±0.0009

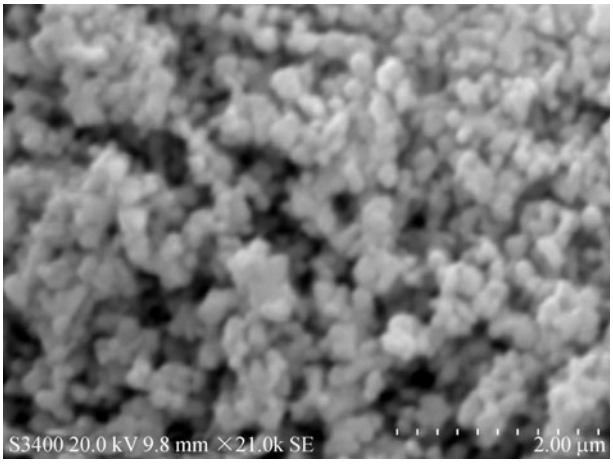

Fig. 3 SEM image of the Cu-doped ZnO sample $Zn_{0.92}Cu_{0.08}O$ annealed at 500°C.

The emission properties of the nanocrystalline Cu-doped ZnO samples were studied at room temperature using a xenon laser of 320 nm as the excitation source. Figure 4 shows the PL spectra of $Zn_{1-x}Cu_xO$ (x = 0.02, 0.04, 0.06, 0.08) nanoparticles annealed at 500°C. From Fig. 4 we observe a strong near-band-edge (NBE) ultraviolet (UV) band at 413 nm (3.00 eV) and the defect related visible emissions: a weak blue band at 452 nm (2.74 eV), a weak blue–green band at 493 nm (2.51 eV) and a strong green band at 549 nm (2.26 eV).

The origin of NBE UV emission is attributed to the recombination of free excitons through an exciton–exciton collision process [17]. The inset of Fig. 4 shows the red shift in the UV emission peak with increasing the copper content in ZnO. The red shift may be ascribed to the

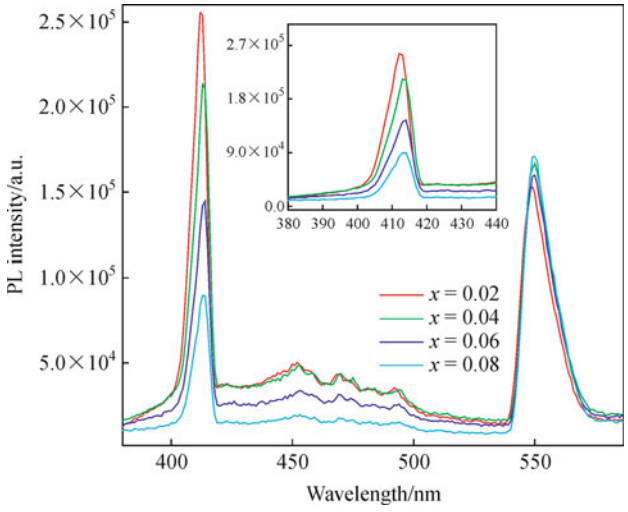

Fig. 4 PL spectra of Cu-doped ZnO nanoparticles annealed at 500°C.

generation of copper impurity levels with increasing the copper concentration in ZnO. It is generally accepted that the visible emissions are attributed to the intrinsic defects and oxygen vacancies in ZnO nanomaterials and the emission results from the radiative recombination of a photogenerated hole with an electron occupying the oxygen vacancy [18–21]. The weak blue and weak blue–green emission results from the deep-level defect emissions are possibly due to surface defects in the ZnO powders [22]. The deep-level emission (DLE) or green emission is caused by the impurities and structural defects in the crystal, for example oxygen vacancy and zinc interstitials [23–24]. The green band emission corresponds to the singly ionized oxygen vacancy in ZnO and results from the recombination of photo generated hole with the single ionized charge state of this defect [25–27].

The intensity variation of UV and visible emissions with increasing the copper concentration in ZnO is attributed to the radiative recombination from the deep levels, surface state levels to conduction band. The green emission intensity is high compared to other visible emissions, which may be due to the high density of oxygen vacancies during the synthesis of the Cu-doped ZnO samples. The Cu-doping induces a decrease in blue and blue–green luminescence intensity while the green emission intensity slightly increases with the Cu-doping in ZnO nanoparticles, indicating that the Cu-doping suppresses the surface states effectively and enhances the oxygen vacancies. Thus, the red shift in the UV emission and the enhancement of oxygen vacancies with increasing the copper content in ZnO indicate the copper ion substitution at Zn site in the lattice.

EPR spectra were used to detect the presence of copper in the nanocrystals. EPR spectral analysis of the Cu-doped ZnO nanocrystals was recorded at room temperature, on a JEOL JES-TE100 ESR spectrometer operating at X-band frequency 9.38653 GHz with microwave power of 1.00 mW in the field range of 0–200 mT, having a 100 kHz field modulation to obtain the first derivative.

Figure 5 shows the room-temperature EPR spectra of $Zn_{1-x}Cu_xO$ (x = 0, 0.02, 0.04, 0.06, 0.08) nanoparticles annealed at 500°C. EPR spectral analysis of ZnO explains the exchange interaction and the defect centers in ZnO [28–29]. The EPR spectra of the samples show a broad signal with anisotropy similar to that of the bulk [30]. Generally EPR powder spectrum of copper gives four lines corresponding to the parallel hyperfine splitting of the copper nucleus (I = 3/2). The presence of the single broad EPR signal suggests that there may be attributed to the ferromagnetic resonance (FMR) arising from the exchange interactions within the copper ions that result in the occurrence of long range ferromagnetic ordering [31].

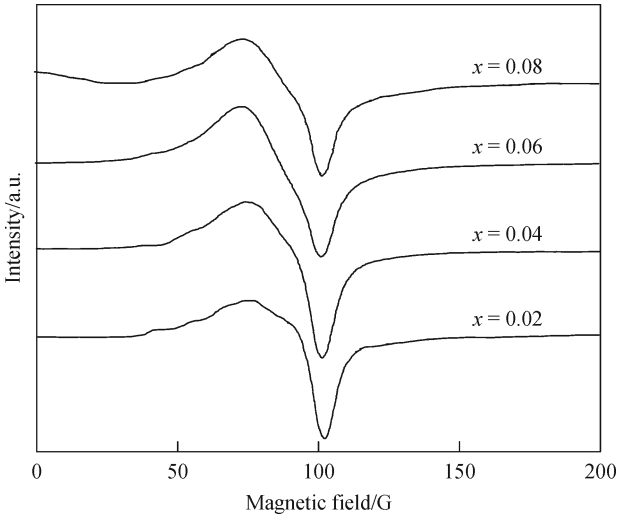

Fig. 5 EPR spectra of Cu-doped ZnO nanoparticles annealed at 500°C.

From the EPR spectra, the parameters g, linewidth (G) and spin–spin relaxation time (t) calculated are given in Table 2. The increase in linewidth with increasing the copper concentration may be due to the exchange or dipolar interaction between the copper ions. The gradual decrease in relaxation time with the increase of the copper concentration is attributed to the decrease in the particle size. It is in agreement with the XRD results that the particle size decreases when the copper content is enhanced

Table 2 EPR parameters of Cu-doped ZnO nanoparticles annealed at 500°C

Copper concentration, x	g-value	Linewidth, G	Spin–spin relaxation time, t /(10^{-10} s)
0.02	2.2968	36.375	0.774
0.04	2.2895	37.500	0.764
0.06	2.2871	38.125	0.752
0.08	2.2847	40.000	0.717

in ZnO. Thus the EPR study on ZnO:Cu nanoparticles confirms that Cu(II) ions are doped substitutionally in ZnO and enhance the non-radiative excitonic transitions.

In summary, Cu-doped ZnO nanoparticles were synthesized using a novel auto-combustion method and exhibit the wurtzite structure. However, when the copper content is $\geqslant$6 mol.%, the CuO phase appears due to the restricted solubility limit of Cu in ZnO. With increasing the copper concentration, the NBE emission in UV region shows a red shift, which indicates that copper ions are substituted in ZnO lattice sites. EPR study on ZnO:Cu nanoparticles confirms that Cu(II) ions are doped substitutionally in ZnO and enhance the non-radiative excitonic transitions.

Acknowledgements Authors wish to express their sincere gratitude to Central Instrumentation Facility, Pondicherry University, for providing SEM and PL measurements. Authors would like to thank the Department of Physics, Pondicherry University for providing XRD measurements and Department of Chemistry, Pondicherry University for providing EPR measurements.

References

[1] Norris D J, Yao N, Charnock F T, et al. High-quality manganese-doped ZnSe nanocrystals. Nano Letters, 2001, 1(1): 3–7

[2] Zhang Q X, Yu K, Bai W, et al. Synthesis, optical and field emission properties of three different ZnO nanostructures. Materials Letters, 2007, 61(18): 3890–3892

[3] Lieber C M. One-dimensional nanostructures: Chemistry, physics & applications. Solid State Communications, 1998, 107(11): 607–616

[4] Ryu Y, Lee T-S, Lubguban J A, et al. Next generation of oxide photonic devices: ZnO-based ultraviolet light emitting diodes. Applied Physics Letters, 2006, 88(24): 241108 (3 pages)

[5] Law M, Greene L E, Johnson J C, et al. Nanowire dye-sensitized solar cells. Nature Materials, 2005, 4(6): 455–459

[6] Sima M, Enculescu I, Sima M, et al. ZnO:Mn:Cu nanowires prepared by template method. physica status solidi (b), 2007, 244 (5): 1522–1527

[7] Wang Y S, Thomas P J, O'Brien P. Optical properties of ZnO nanocrystals doped with Cd, Mg, Mn, and Fe ions. The Journal of Physical Chemistry B, 2006, 110(43): 21412–21415

[8] Park Y R, Choi S L, Lee J H, et al. Ferromagnetic properties of Ni-doped rutile $TiO_{2-\delta}$. Journal of the Korean Physical Society, 2007, 50(3): 638–642

[9] Liu C, Yun F, Morkoç H. Ferromagnetism of ZnO and GaN: A review. Journal of Materials Science: Materials in Electronics, 2005, 16(9): 555–597

[10] Huang L M, Rosa A L, Ahuja R. Ferromagnetism in Cu-doped ZnO from first-principles theory. Physical Review B: Condensed Matter and Materials Physics, 2006, 74(7): 075206 (6 pages)

[11] Bhargava R N, Chhabra V, Som T, et al. Quantum confined atoms of doped ZnO nanocrystals. physica status solidi (b), 2002, 229(2): 897–901

[12] Chakraborti D, Ramachandran S, Trichy G, et al. Magnetic, electrical, and microstructural characterization of ZnO thin films codoped with Co and Cu. Journal of Applied Physics, 2007, 101 (5): 053918 (7 pages)

[13] Ni Y H, Cao X F, Wu G G, et al. Preparation, characterization and property study of zinc oxide nanoparticles via a simple solution-combusting method. Nanotechnology, 2007, 18(15): 155603 (4 pages)

[14] Jimenez-Gonzalez A E. Modification of ZnO thin films by Ni, Cu, and Cd doping. Journal of Solid State Chemistry, 1997, 128(2): 176–180

[15] Lee H-J, Kim B-S, Cho C R, et al. A study of magnetic and optical properties of Cu-doped ZnO. physica status solidi (b), 2004, 241 (7): 1533–1536

[16] Shannon R D. Revised effective ionic radii and systematic studies of interatomic distances in halides and chalcogenides. Acta Crystallographica Section A: Crystal Physics, Diffraction, Theoretical and General Crystallography, 1976, 32: 751–767

[17] Wang H, Wang H B, Yang F J, et al. Structure and magnetic properties of $Zn_{1-x}Co_xO$ single-crystalline nanorods synthesized by a wet chemical method. Nanotechnology, 2006, 17(17): 4312–4316

[18] Li C, Fang G, Fu Q, et al. Effect of substrate temperature on the growth and photoluminescence properties of vertically aligned ZnO nanostructures. Journal of Crystal Growth, 2006, 292(1): 19–25

[19] Sun Y, Ndifor-Angwafor N G, Riley D J, et al. Synthesis and photoluminescence of ultra-thin ZnO nanowire/nanotube arrays formed by hydrothermal growth. Chemical Physics Letters, 2006, 431(4–6): 352–357

[20] Ryu Y R, Zhu S, Budai J D, et al. Optical and structural properties of ZnO films deposited on GaAs by pulsed laser deposition. Journal of Applied Physics, 2000, 88(1): 201–204

[21] Chen Y, Hong K, Ko H J, et al. Plasma-assisted molecular-beam

epitaxy of ZnO epilayers on atomically flat $MgAl_2O_4$(111) substrates. Applied Physics Letters, 2000, 76(2): 245–247

[22] Wang J, Gao L. Hydrothermal synthesis and photoluminescence properties of ZnO nanowires. Solid State Communications, 2004, 132(3–4): 269–271

[23] Vanheusden K, Warren W L, Seager C H, et al. Mechanisms behind green photoluminescence in ZnO phosphor powders. Journal of Applied Physics, 1996, 79(10): 7983–7990

[24] Korsunska N O, Borkovska L V, Bulakh B M, et al. The influence of defect drift in external electric field on green luminescence of ZnO single crystals. Journal of Luminescence, 2003, 102–103: 733–736

[25] Monticone S, Tufeu R, Kanaev A V. Complex nature of the UV and visible fluorescence of colloidal ZnO nanoparticles. The Journal of Physical Chemistry B, 1998, 102(16): 2854–2862

[26] Yao B D, Chan Y F, Wang N. Formation of ZnO nanostructures by a simple way of thermal evaporation. Applied Physics Letters, 2002, 81(4): 757–759

[27] Xu C X, Sun X W, Zhang X H, et al. Photoluminescent properties of copper-doped zinc oxide nanowires. Nanotechnology, 2004, 15 (7): 856–861

[28] Vlasenko L. Point defects in ZnO: Electron paramagnetic resonance study. Physica B: Condensed Matter, 2009, 404(23–24): 4774–4778

[29] Liu W K, Whitaker K M, Smith A L, et al. Room-temperature electron spin dynamics in free-standing ZnO quantum dots. Physical Review Letters, 2007, 98(18): 186804 (4 pages)

[30] Kannappan R, Mahalakshmy R, Rajendiran T M, et al. Magnetic, catalytic, EPR and electrochemical studies on binuclear copper(II) complexes derived from 3,4-disubstituted phenol. Journal of Chemical Sciences, 2003, 115(1): 1–14

[31] Viswanatha R, Chakraborty S, Basu S, et al. Blue-emitting copper-doped zinc oxide nanocrystals. The Journal of Physical Chemistry B, 2006, 110(45): 22310–22312